Theoretical studies of epitaxially grown Co and Ni thin films on (111) metallic substrates

M. Zelený[1,2,3] and M. Šob[2,3]
[1]*Faculty of Chemistry, Brno University of Technology, Brno, Czech Republic*
[2]*Department of Chemistry, Faculty of Science, Masaryk University, Brno, Czech Republic*
[3]*Institute of Physics of Materials, Academy of Sciences of the Czech Republic, Brno, Czech Republic*
(Received 9 February 2008; revised manuscript received 14 March 2008; published 24 April 2008)

Total energies of hcp and trigonally distorted fcc Co and Ni are studied from first principles. Regions of stability of these structures are found and the behavior of the total energies is used to explain and predict the lattice parameters and magnetic states of Co and Ni thin films on various (111) substrates. The stresses needed to keep the thin films coherent with the substrates are also determined. The theoretical results agree surprisingly well with available experimental data.

DOI: 10.1103/PhysRevB.77.155435 PACS number(s): 68.35.−p, 71.15.Nc, 75.70.Ak

I. INTRODUCTION

Transition-metal thin films and multilayers have attracted a lot of interest because of their technological importance in data storage and sensor applications and in fundamental research of magnetism.

Bulk Co exists in two ferromagnetic thermodynamically stable phases at ambient pressure: hcp α-Co below 388 °C and fcc β-Co above 450 °C. In the case of Ni, only the fcc modification is stable, but Ni with a hcp structure was observed under special conditions.[1] It turns out that in most cases, Ni and Co thin films exhibit structures similar to those in the bulk, i.e., no major reconstruction usually takes place. For example, only trigonally distorted fcc films of Ni were observed[2,3] and cobalt thin films with a hcp structure[4] as well as those with a trigonally distorted fcc structure[5] were found on fcc (111) substrates. In some cases, both structures were reported.[6] Thin films of both metals with the bcc structure were prepared on GaAs(001) substrate.[7,8]

The goal of this contribution is to advance our fundamental understanding of epitaxial growth of Co and Ni thin films on various fcc (111) substrates. For this purpose, we employ *ab initio* electronic structure calculations of the total energy of and the stress on biaxially deformed bulk materials. Namely, pseudomorphic overlayers adopt the lattice dimensions of a fcc substrate on the (111) plane and relax the interlayer distance [the description of this situation for (001) substrates and a more detailed discussion can be found, e.g., in Ref. 9]. On the atomic planes of the film parallel to the interface, there is a stress σ^{epi} that keeps the structure of the film and of the substrate coherent, and the stress perpendicular to these planes vanishes due to the relaxation of the interlayer distance d (Fig. 1). On the (111) surface, there are two possible stackings of the layers in the film: *ABABAB*…, which gives the hcp structure, and *ABCABC*…, which provides the trigonally distorted fcc structure. The nearest-neighbor distance D_{NN} in the (111) plane of the fcc substrate is equal to $a_{\mathrm{sub}}\sqrt{2}/2$, where a_{sub} is the lattice constant of the substrate. If there is a large difference between the lattice dimensions of the substrate and the material of the film (lattice mismatch), the stress σ^{epi} on the planes parallel to the interface will be too large. As a consequence, the film may become incoherent, i.e., the distance of the nearest neighbors in the (111) overlayers (for the trigonally distorted fcc films) or (0001) overlayers (for the hcp films) d_{nn} differs from D_{NN}. Such a film cannot be pseudomorphically grown and usually has a structure similar to the ground-state structure of the bulk of the film material. The limit of the stability of coherent films is set by the maximum of the stress on the planes parallel to the interface as a function of D_{NN}, which corresponds to the inflection point on the dependence of total energy on D_{NN} [the stress σ^{epi} is calculated as a derivative of the total energy with respect to strain in the (111) or (0001) plane of the bulk and the maximum value of this derivative is found at the inflection point].

Our investigations allow us to elucidate the structure of Co and Ni thin films on various fcc (111) substrates from first principles. We explain why some of those films exhibit the hcp structure and some of them exhibit the trigonally distorted fcc structure and for which substrate the film may be coherent. A similar study was performed by Kraft *et al.*[10] for hcp and fcc iron thin films. However, those authors did

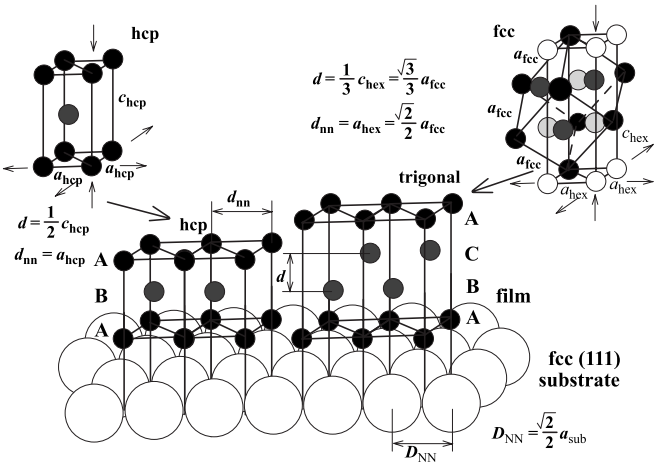

FIG. 1. Epitaxial growth of the hcp (left) and trigonally distorted fcc (right) thin films on the (111) fcc substrate. As shown in the upper right corner, the fcc cell may also be characterized by hexagonal coordinates (a_{hex}, c_{hex}). The distance between the (111) or (0001) planes in the film, the nearest-neighbor distance in the (111) plane of the fcc substrate, and the nearest-neighbor distance in the (111) or (0001) overlayers are denoted as d, D_{NN}, and d_{nn}, respectively.

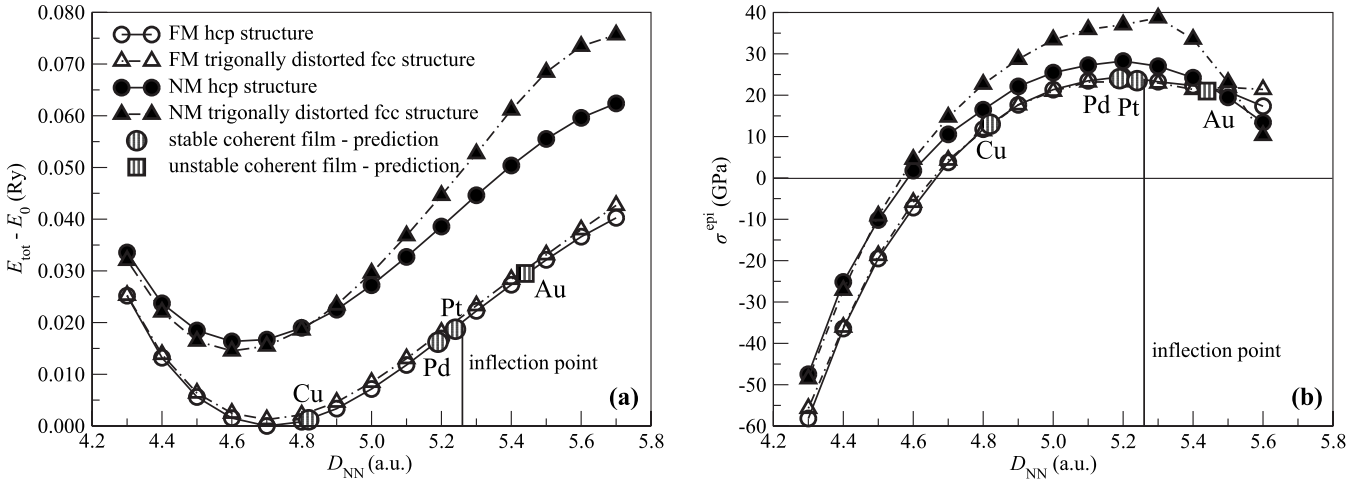

FIG. 2. (a) Total energy of biaxially deformed bulk Co and (b) the corresponding stress on the (111) and (0001) planes as a function of nearest-neighbor distance D_{NN} in the fcc (111) substrate. The empty symbols correspond to FM states and the full symbols correspond to NM states. The striped symbols denote our predictions of the structures and coherence of Co thin films on different fcc (111) substrates. The inflection point (marked by a thin full vertical line) is shown only for the most stable structures.

not discuss the coherence of thin films on various substrates and their calculations were accomplished with the help of the local spin-density approximation, which does not provide correct energetics for ferromagnetic 3*d* metals. Another detailed study about the stability of deformed structures of hcp Co was performed by Guo *et al.*,[11] but those authors did not consider the trigonally distorted fcc structures.

II. METHODS

To simulate the epitaxial growth, we first calculate the total energy of the film material (i.e., Co and Ni) in equilibrium hcp and fcc structures in both nonmagnetic (NM) and ferromagnetic (FM) states. Here, the transformation of a fcc cell to hexagonal coordinates is useful (Fig. 1). Then, in the second step, we perform some elongation or contraction (biaxial deformation) of the bulk crystal along two perpendicular directions [along the (111) plane for the fcc structure or along the (0001) plane for the hcp structure] by a fixed amount of ε that provides the same nearest-neighbor distance d_{nn}, as is found in the (111) plane of substrate D_{NN}. For each ε, we minimize the total energy, relaxing the stress in the direction perpendicular to the (111) or (0001) planes and, thus, determining the equilibrium interlayer distance d at this $d_{nn}=D_{NN}$. This is a very simple model, which can be used for film thicknesses that are neither too thin nor too thick (between about 3 and 12 monolayers), but it turns out that this model is quite realistic. In the past, Friák *et al.*[9] and Jona *et al.*[12] used a similar approach for investigations of iron thin films on (001) substrates and of hcp Cu on W(001) surface, respectively.

For the total-energy calculations, we employ the full-potential linearized augmented plane wave method, which is incorporated in the WIEN2K code,[13] and the generalized gradient approximation.[14] The muffin-tin radius of atoms of 2.0 a.u. is kept constant for all calculations, the number of **k** points in the irreducible Brillouin zone is equal to 3600, and the product of the muffin-tin radius and the maximum reciprocal space vector, $R_{MT}k_{max}$, is equal to 9. For nickel, the maximum value of l for the waves inside the atomic spheres l_{max} and the size of the largest reciprocal vector **G** in the charge Fourier expansion G_{max} are set to 9 and 16, respectively. For cobalt, l_{max} is set to 11 and G_{max} is set to 16. The augmented plane wave plus local-orbital extension was used for a correct treatment of 3*p* semicore states.[15] The energy convergence criterion was 1×10^{-6} Ry/atom, and on the basis of the convergence tests with respect to the number of the **k** points, the error in calculated total energies may be estimated to be less than 5×10^{-5} Ry/atom. This corresponds to the error bar of ±0.02 a.u. in the values of D_{NN} and d displayed in Figs. 2(a) and 3(a). Some experimental papers report an error bar of a similar size,[4,16] but some do not mention the experimental errors at all. Our error bar is smaller than the size of the symbols that are used in Figs. 2(a), 3(a), and 5.

III. RESULTS AND DISCUSSION

The total energy of biaxially deformed bulk Co as a function of D_{NN} is shown in Fig. 2(a). The triangles correspond to trigonally distorted fcc structures (with the layer sequence *ABCABC*… in Fig. 1) and the circles correspond to hcp structures (with the layer sequence *ABABAB*… in Fig. 1). The empty symbols correspond to FM states and the full symbols to NM states. There are several interesting points on these dependences. Each curve has the global minimum, which corresponds to the equilibrium state. The equilibrium state with the lowest energy is the FM hcp ground state of Co. The structural energy difference between the FM hcp and FM fcc structures at this point is 1.1 mRy/atom. The total energies of hcp structures are lower than the energies of trigonally distorted fcc structures, which means that hcp phases are energetically more favorable within the whole interval of D_{NN} that is studied. The second interesting point on

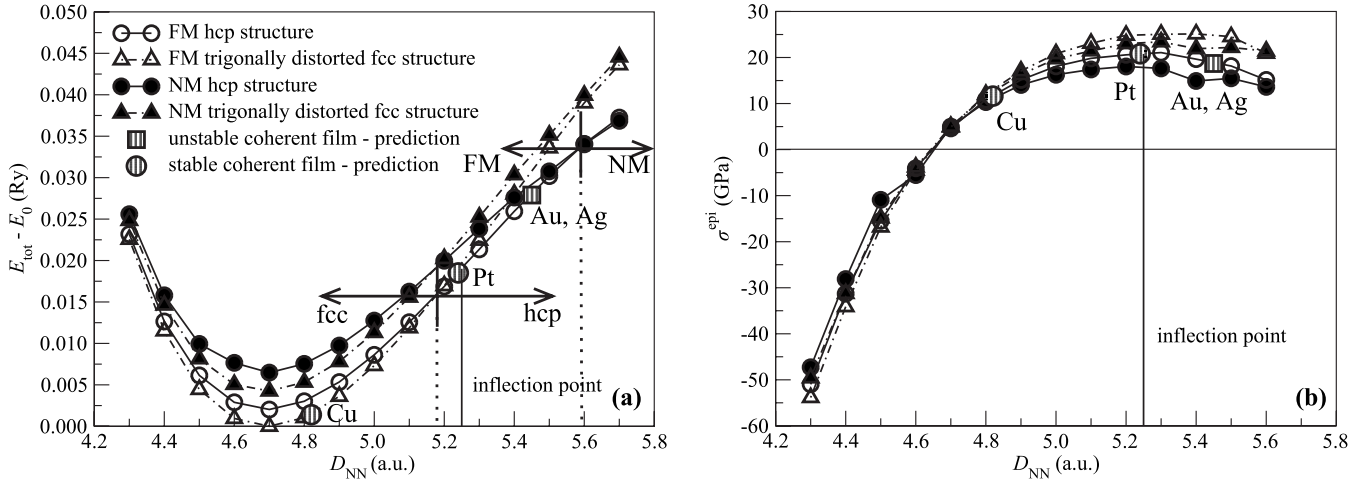

FIG. 3. (a) Total energy of biaxially deformed bulk Ni and (b) the corresponding stress on the (111) and (0001) planes as a function of nearest-neighbor distance D_{NN} in the fcc (111) substrate. The empty symbols correspond to FM states and the full symbols correspond to NM states. The striped symbols denote our predictions of the structures and coherence of Ni thin films on different fcc (111) substrates. The inflection point (marked by a thin full vertical line) is shown only for the most stable structures. The thin dashed vertical lines in (a) indicate the intersection of curves for the hcp and trigonally distorted fcc FM states (left line) and the hcp FM and hcp NM states (right line).

each curve is the inflection point. The inflection point with the lowest energy corresponds to the maximum strain on the planes parallel to the interface and to maximum D_{NN} (5.26 a.u.), at which a Co thin film may be expected to be coherent.

The calculated tensile stresses on the (111) and (0001) planes of biaxially deformed fcc and hcp bulk Co are shown in Fig. 2(b). In the equilibrium state, the stress acting on the (111) and (0001) planes of the bulk crystals is equal to zero. When we apply some elongation along perpendicular directions on the (111) or (0001) planes (i.e., we increase D_{NN}), the stress acting on these planes increases as well. The maximum value of the stress on the (0001) plane for FM Co with the hcp structure is equal to 23.4 GPa [see Fig. 2(b)]; it may be considered as a theoretical strength limit. The values that are shown in Fig. 2(b) for D_{NN}, which are less or equal to 5.26 a.u., represent the stresses needed to keep the Co thin films coherent with the substrate.

A hcp structure was experimentally found in Co films on a Cu(111) substrate[17] with D_{NN}=4.82 a.u. [see the lowest striped circle in Fig. 2(a) and Table I], and islands with trigonally distorted fcc structures were also reported.[6] This is due to a small structural energy difference between the hcp and fcc phases of Co, so a transition between these phases is very easy. To the best of our knowledge, the only coherent films of cobalt were found on a Cu(111) substrate. Our calculations also predict coherent Co layers on Pt(111) and Pd(111) because D_{NN} for these substrates (5.19 and 5.24 a.u., respectively) are smaller than the value corresponding to the inflection point (5.26 a.u.) [see Fig. 2(a)]. However, let us note that the stresses needed to keep these films coherent are very large. They are quite close to the theoretical strength limit [Fig. 2(b)], which may make the formation of coherent layers difficult. Indeed, the experimentally prepared films on these substrates are incoherent. Co thin films on Pd(111) substrate do not have clearly determined structure and lattice parameters,[16,18] and the structure of Co thin films on Pt(111) strongly depends on the way of preparation.[19,20] The other reasons for the difference between our prediction and experiment may be the diffusion of Pt or Pd into the Co film and

TABLE I. A comparison of theoretical results and experimental data for Co films on Cu (Ref. 17), Pd (Ref. 16), Pt (Refs. 5 and 19), and Au (Ref. 4) substrates and Ni films on Cu (Ref. 6), Pt (Ref. 21), and Au and Ag (Ref. 22) substrates. Predictions of interlayer distance d are shown only for the coherent films.

			Theor.			Expt.			
Film/substrate	a_{sub} (a.u.)	D_{NN} (a.u.)	d (a.u.)	Structure	Film	d (a.u.)	d_{nn} (a.u.)	Structure	Film
Co/Cu(111)	6.82	4.82	3.78	hcp	Coherent	3.82	4.82	hcp	Coherent
Co/Pd(111)	7.34	5.19	3.59	hcp	Coherent	3.72	4.91	hcp/fcc	Incoherent
Co/Pt(111)	7.40	5.24	3.56	hcp	Coherent	3.68	4.99	hcp/fcc	Incoherent
Co/Au(111)	7.69	5.44		hcp	Incoherent	3.84	4.74	hcp	Incoherent
Ni/Cu(111)	6.82	4.82	3.80	fcc	Coherent	3.82	4.82	fcc	Coherent
Ni/Pt(111)	7.40	5.24	3.55	fcc/hcp	Coherent	3.61	5.24	fcc	Coherent
Ni/Au(111)	7.69	5.44		fcc	Incoherent	3.78	4.74	fcc	Incoherent
Ni/Ag(111)	7.71	5.45		fcc	Incoherent	3.78	4.74	fcc	Incoherent

the formation of alloys based on CoPt.[5] For Co on a Au(111) substrate (D_{NN}=5.44 a.u., behind the inflection point), we predict an unstable coherent film, which therefore cannot be observed in experiment but rather an incoherent film may be expected. Indeed, in Ref. 4, an incoherent Co film was found. For the prediction of the parameters of incoherent films, our present approach cannot be employed.

Nickel films behave quite differently [Fig. 3(a)]. The structural energy difference between the hcp FM and the fcc FM Ni at the energy minimum amounts to 2.0 mRy/atom, which is about double of the value for Co. The maximum value of D_{NN}, at which the Ni film may be expected to be coherent (position of the inflection point) is equal to 5.25 a.u. An interesting place on these dependences [the open symbols in Fig. 3(a)] is a crossing point between the curves for the hcp and trigonally distorted fcc FM states at 5.18 a.u. At this position, a phase transition between these structures may be expected. A second phase transition, i.e., from the hcp FM phase to the hcp NM phase, might occur for D_{NN} equal to 5.59 a.u. However, this point lies outside of the stability region of Ni films on fcc (111) substrates, quite far behind the inflection point. The corresponding stresses on Ni thin films are shown in Fig. 3(b). The maximum value of the stress on the (0001) plane for FM Ni with the hcp structure is equal to 20.4 GPa.

It may be seen from Fig. 3(a) that the fcc layer stacking (*ABCABC*…) in the Ni overlayers is stable up to D_{NN} equal to 5.18 a.u. This is in good agreement with the experimental data for Ni film on Cu(111) (Ref. 6) substrates (see also Table I). If the substrates have a D_{NN} that is larger than 5.18 a.u. but is lower or equal to 5.25 a.u. (the inflection point), the film should exhibit the hcp layer stacking (*ABAB*…). The value of D_{NN} of 5.24 a.u. for the Pt(111) substrate is nearly equal to 5.25 a.u. so that we can expect hcp islands in the Ni films here. Experimentally prepared Ni films on Pt(111) substrates are coherent, although the stresses needed to keep the film coherent are close to the theoretical strength limit [see Fig. 3(b)], but they exhibit the trigonally distorted fcc structure.[21] This discrepancy can again be explained by a small energy difference between the hcp and fcc structures at this point. Au and Ag substrates have a larger D_{NN} than the value corresponding to the inflection point and our calculations predict unstable coherent hcp Ni films on these substrates, which again should not exist in reality. Indeed, in experiment, incoherent thin films were observed that had a structure similar to fcc Ni in the ground state.[22]

The magnetic moments of biaxially deformed bulk Co and Ni as a function of D_{NN} are shown in Fig. 4. In both cases, we may observe a slight and nearly linear increase in magnetic moments with increasing D_{NN}, which is also connected with increasing atomic volume. However, increasing D_{NN} is also accompanied by a decreasing interlayer distance d (see Fig. 5), and at a certain configuration, d is too small to keep the ferromagnetic order. This configuration was found for Ni with the hcp structure at D_{NN}=5.59 a.u. and d=3.20 a.u. [see Fig. 5(b)]. Here, the magnetic moment goes to zero and Ni becomes nonmagnetic, which is accompanied by the crossing of energies for ferromagnetic and nonmagnetic states in Fig. 3(a). However, this point lies outside of the stability region of Ni films on the fcc(111) substrates.

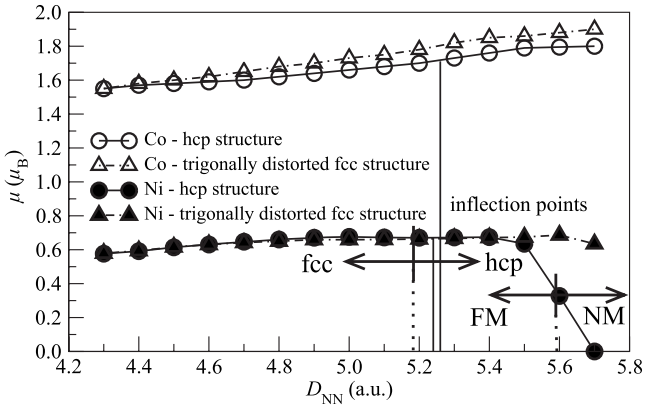

FIG. 4. Magnetic moments of biaxially deformed bulk Co and Ni as a function of nearest-neighbor distance D_{NN} in the fcc (111) substrate. The empty symbols correspond to Co and the full symbols to Ni. The inflection points (marked by the thin full vertical lines) are shown only for the most stable structures. The thin dashed vertical lines indicate the intersection of energies of hcp and trigonally distorted fcc FM Ni (left line) and of hcp FM and hcp NM Ni (right line) displayed in Fig. 3(a).

Let us note that the magnetic moments shown in Fig. 4 correspond to those of the deformed bulk material. Therefore, they should be considered rather as lower limits of magnetic moments in thin films, as, in reality, when the atoms are closer to the surface of the film, it may be expected that the size of their magnetic moments will be larger due to a reduced coordination.

The total energies of bulk Co and Ni as a function of D_{NN} and interlayer distance d are displayed in Figs. 5(a) and 5(b). Only states with the minimum energy are shown. In Fig. 5(a), the thick line marks the phase boundary between the hcp FM phase and the trigonally distorted fcc FM phase. In Fig. 5(b), the central part corresponds to the trigonally distorted fcc FM states. On both sides, we may observe hcp FM regions, and for the lowest values of the interlayer distance d, a hcp NM region is present. We also show the lowest energies from Figs. 2(a) and 3(a) as well as the experimental and predicted lattice parameters of Co and Ni films. A short dashed line indicates the boundary up to which the films should be coherent with the substrates.

A comparison of the numerical values of calculated and experimental lattice parameters of Co and Ni films on fcc (111) substrates is given in Table I. It can be seen from Table I and from Fig. 5 that our results are in a surprisingly good agreement with available experimental data. For Co/Cu(111), we have a nearly perfect fit. For Co/Au(111), we predict an incoherent film, which is in agreement with the observations. The theoretical points corresponding to Co/Pd(111) and Co/Pt(111) films are just below our predicted stability limit [see Fig. 5(b)] and the experimentally observed incoherent films may be due to imperfections, which might shift the corresponding energies above this limit. For Ni/Cu(111) and Ni/Pt(111), again we have a nearly perfect fit, although the energy of Ni/Pt(111) films lies just below the stability limit. For Ni/Au(111) and Ni/Ag(111), we predict incoherent films, which is again in agreement with experimental findings.

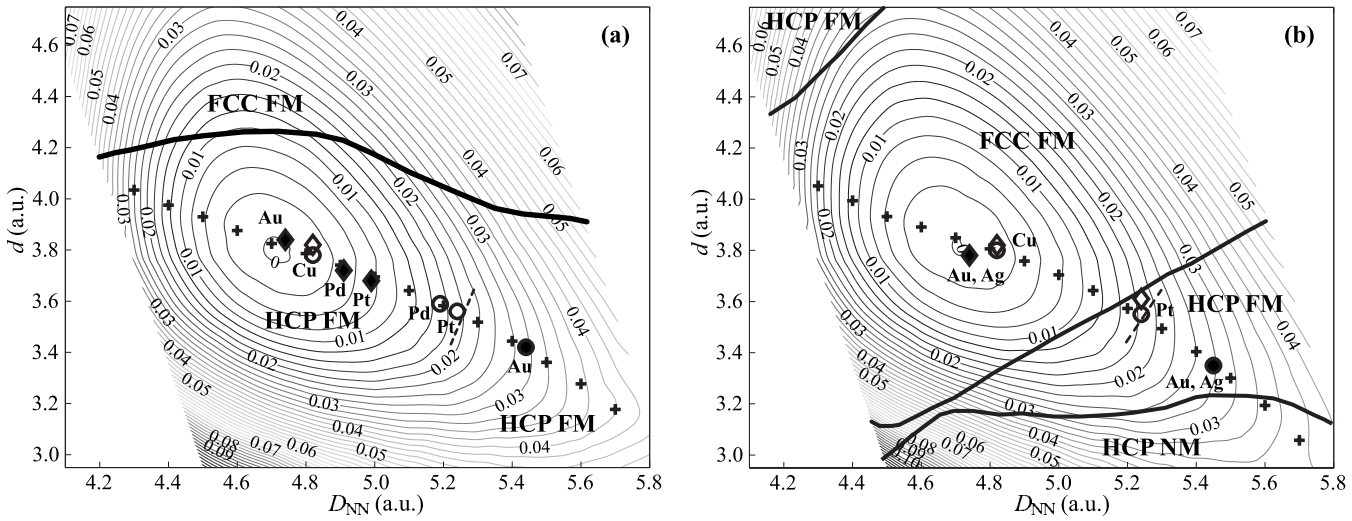

FIG. 5. Total energies of biaxially deformed bulk (a) Co and (b) Ni as a function of nearest-neighbor distance D_{NN} and interlayer distance d. Only states with the minimum energy are shown. The contour interval is 2.5 mRy/atom. The thick lines show the phase boundaries between the different phases. The crosses correspond to the lowest energies from Figs. 2(a) and 3(a). The dashed lines perpendicular to these curves mark the boundaries up to which the films should be coherent with the substrates. The empty and the full diamonds indicate the experimental lattice parameters of coherent and incoherent films, respectively. For incoherent films, we employ the experimental value of the nearest-neighbor distance in the overlayers d_{nn} (see Table I). The empty and the full circles correspond to our predictions of the lattice parameters for stable and unstable coherent films, respectively.

Let us note that the curves in Figs. 2(a) and 3(a) may be used for the prediction of stability and magnetic state of Co and Ni thin films on other (111) fcc substrates.

To check the validity of the our approach, we performed supercell calculations by using six layers of Ni or Co on a substrate with a fixed D_{NN} in the bottom layer and relaxed the interlayer distances. It turns out that both the bulk and the supercell calculations predict the same energetically most favorable structure and the interlayer distances in the interior of the film agree with those from the bulk calculations within 1% for the case of nickel overlayers and within 1.5% for the case of most cobalt overlayers.

IV. CONCLUSIONS

We have calculated the total energies of bulk Co and Ni as a function of the nearest-neighbor distance D_{NN} in the (111) plane of the substrate in the trigonally distorted fcc structure and hcp structure, identified phase boundaries between these two structures, and applied these results to elucidate the atomic configuration and magnetic orders of Co and Ni thin films on fcc(111) substrates. We have also determined stresses needed to keep the Co and Ni thin films coherent with the substrate. The maximum values of these stresses correspond to the inflection points on the dependences of total energy on D_{NN} and indicate the limits of stability of the coherent films.

Our predictions for Co and Ni films are in good agreement with available experimental data. A discrepancy found for the Co/Pd(111) and Co/Pt(111) films is probably due to a small structural energy difference between the hcp and fcc structures. Of course, some deviations between the calculated results and experiment may also be due to the simplicity of our model of epitaxial growth, which cannot include some effects as a chemical reaction with the substrate or diffusion. However, it seems that our approach captures most of the underlying physics of the phenomenon studied and provides correct limits for coherent growth of Ni and Co overlayers on various (111) substrates.

ACKNOWLEDGMENTS

This research was supported by the Grant Agency of the Czech Republic (Projects No. 202/06/1509 and No. 106/05/H008), by the Grant Agency of the Academy of Sciences of the Czech Republic (Project No. IAA1041302), and by the Research Projects No. AV0Z20410507 and No. MSM0021622410. The use of the computer facilities at the MetaCenter of the Masaryk University, Brno, is acknowledged.

[1] J. Vergara and V. Madurga, J. Mater. Res. **17**, 2099 (2002).
[2] D. W. Gidley, Phys. Rev. Lett. **62**, 811 (1989).
[3] M. Sambi, E. Pin, and G. Granozzi, Surf. Sci. **340**, 215 (1995).
[4] N. Marsot, R. Belkhou, H. Magnan, P. Le Fevre, C. Guillot, and D. Chandesris, Phys. Rev. B **59**, 3135 (1999).
[5] M. Galeotti, A. Atrei, U. Bardi, B. Cortigian, G. Rovida, and M. Torrini, Surf. Sci. **297**, 202 (1993).
[6] F. Huang, M. T. Kief, G. J. Mankey, and R. F. Willis, Phys. Rev.

B **49**, 3962 (1994).
[7] C. S. Tian *et al.*, Phys. Rev. Lett. **94**, 137210 (2005).
[8] G. A. Prinz, Phys. Rev. Lett. **54**, 1051 (1985).
[9] M. Friák, M. Šob, and V. Vitek, Phys. Rev. B **63**, 052405 (2001).
[10] T. Kraft, M. Methfessel, M. van Schilfgaarde, and M. Scheffler, Phys. Rev. B **47**, 9862 (1993).
[11] H. B. Guo, J. H. Li, L. T. Kong, and B. X. Liu, Phys. Rev. B **72**, 132102 (2005).
[12] F. Jona, X. Z. Ji, and P. M. Marcus, Phys. Rev. B **68**, 172101 (2003).
[13] P. Blaha, K. Schwarz, G. K. H. Madsen, D. Kvasnicka, and J. Luitz, *WIEN2k, An Augmented Plane Wave Plus Local Orbitals Program for Calculating Crystal Properties* (Karlheinz Schwarz, Technical University of Vienna, Vienna, 2001).
[14] J. P. Perdew, K. Burke, and M. Ernzerhof, Phys. Rev. Lett. **77**, 3865 (1996).
[15] S. Cottenier, *Density Functional Theory and The Family of (L)APW-Methods: A Step-by-Step Introduction* (Instituut voor Kern- en Stralingsfysica, K. U. Leuven, Belgium, 2002).
[16] S. K. Kim, Y. M. Koo, V. A. Chernov, and H. Padmore, Phys. Rev. B **53**, 11114 (1996).
[17] P. Le Fevre, H. Magnan, O. Heckmann, V. Briois, and D. Chandesris, Phys. Rev. B **52**, 11462 (1995).
[18] A. Atrei, G. Rovida, M. Torrini, U. Bardi, M. Gleeson, and C. J. Barnes, Surf. Sci. **372**, 91 (1997).
[19] J. Thiele, R. Belkhou, H. Bulou, O. Heckmann, H. Magnam, P. Le Fevre, D. Chandesris, and C. Guillot, Surf. Sci. **384**, 120 (1997).
[20] S. Ferrer, J. Alvarez, E. Lundgren, X. Torrelles, P. Fajardo, and F. Boscherini, Phys. Rev. B **56**, 9848 (1997).
[21] M. Sambi and G. Granozii, Surf. Sci. **400**, 239 (1998).
[22] S. Morin, A. Lachenwitzer, F. A. Möller, O. M. Magnussen, and R. J. Behm, J. Electrochem. Soc. **146**, 1013 (1999).